

A segmentation algorithm for a robotic micro-endoscope for exploration of the spinal cord

Luca Ascari*, Ulisse Bertocchi[§], Cecilia Laschi[†], Cesare Stefanini*, Antonina Starita[§] and Paolo Dario*[†]

*CRIM Lab, Scuola Superiore Sant'Anna, Pisa, Italy

[†]ARTS Lab, Scuola Superiore Sant'Anna, Pisa, Italy

[§]Dept. of Computer Science, University of Pisa, Italy

E-mail:ascari@sss sup.it

Abstract—This paper presents an adaptive segmentation algorithm for endoscopic images. It is part of a complete system for robot-assisted endoscopy of the human sub-arachnoid spinal space. The role of the vision system is to provide a feedback for assisting the navigation of the endoscope and helping avoid damages to delicate tissues. Due to the presence of small blood vessels, nerves, and possible fibrosis, a multi-step approach has been followed for segmentation of the lumen (corresponding to free space for navigation) and the other tissues. *Histogram analysis*, together with *blob analysis* and a modified implementation of the *Convex Hull* algorithm bring to the isolation of the lumen; by means of *adaptive thresholding* nerves are isolated; thresholding on the *hue* and *saturation* helps in recognizing the vessels. A special condition of *dirty lumen* helps in managing doubtful situations.

Experimental trials have been conducted on video streams from endoscopic explorations of animal (pig) spinal cord *in-vivo*. Experimental results show that membranes, vessels, nerves, and lumen are recognized in a reliable way, so as to contribute to robot-assisted endoscopy.

The speed of the processing resulted compatible with an envisaged use in real time support of endoscopic navigation.

I. INTRODUCTION

There are many different pathological diseases affecting the spinal cord. In addition to traumas, which represent the major part, there are aneurysms, tumours, infections, degenerative processes and late surgical complications [1]. Medical imaging is a non invasive diagnostic technique very often exploited. On the other hand, the resolution of the images, with or without contrast media, is still not comparable with the direct vision of the anatomical structures [2]. Often MRI or CT images are not able to provide sufficient useful information for diagnoses [3].

In [4] we described a new active micro-catheter for the exploration of the sub-arachnoid spinal space. The endoscope inside the catheter provides the surgeon with a direct vision of the spinal canal, but poses important safety issues. In fact any contact between the catheter and the delicate structures present in that environment must be avoided. An automatic tool preventing the surgeon from directing the catheter against nerve roots and vessels is an essential component of a medical system for endoscopic exploration of the sub-arachnoid space.

In this paper a collaborative system for endoscopic catheter navigation is presented, based on the segmentation of the images coming from the endoscope. The aim of image segmentation is to divide an image into parts that have a strong

correlation with objects or areas of the real world contained in the image. A *complete segmentation* results in a set of disjoint regions in a biunique relation with the objects in the input image, while in a *partial segmentation* this exact correspondence is not needed. In order to obtain a complete segmentation of the input image, essential for navigation purposes, a specific knowledge of the environment is necessary and must be used in the algorithm. A more detailed description of the subarachnoid spinal space is presented in [4].

To our knowledge, no work has been done in the segmentation of subarachnoid spinal images. Nevertheless many researchers report on the clusterization and segmentation of colonoscopic images, aiming at assisted navigation of an endoscopic robot in the colon.

A technique using the Fourier Transform to identify the lumen location is described by Kwoh et al. [5]. The method, even if effective in identifying the lumen position for a great variety of images, shows a lack of effectiveness when employed on images with artifacts, such as diverticula or pockets on the inner walls.

Khan and Gillies [6] describe a region based segmentation method combined with an edge based approach; one of the limits of this approach is the fixed threshold used for lumen discrimination; some authors ([7], [8]) use Adaptive Progressive Thresholding (APT) to overcome this problem. Performances are good but the computational complexity of this approach is very high.

A faster method to extract the lumen from grayscale endoscopic images is proposed by Kumar et al. [9] and Asari [10]: it consists of a two-phase algorithm; in the first phase, a quasi-region of interest indicating the lumen is extracted, using an APT approach; Differential Region Growing (DRG) is then used to segment the actual lumen.

All the methods presented above can be applied to grayscale images only. Indeed, important information are conveyed by color. A computationally efficient segmentation technique for endoscopic color images is described in [11]: the image is first segmented using a peak-finding algorithm on a 2-D histogram of homogeneity and intensity values, and then the information on the hue is used to complete the process. In our case this approach has proven to fail in the recognition of vessels and nerves inside the lumen.

Krishnan et al. [12] propose a fuzzy rule base approach for

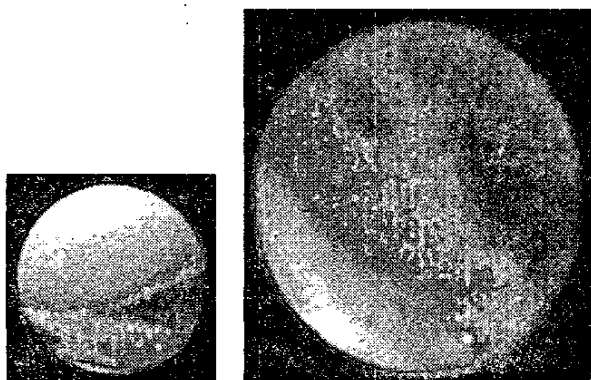
the labelling of colonoscopic images.

In this paper, we describe a segmentation algorithm for color endoscopic images of the spinal canal. From a navigation point of view there are significant differences with colonoscopic images: the lumen is not normally convex and anatomic structures like nerves and blood vessels can exist in front of the camera inside the lumen itself, thus making the development of a reliable segmentation algorithm a challenging task.

Lumen, walls, nerve roots and blood vessels are recognized in real time, thus allowing a thorough understanding of the scene. This is the first step to approach the development of an automatic obstacle-avoidance module for a vision-driven spinal endoscopy system.

II. METHODS AND IMPLEMENTATION

In fig.1, two endoscopic pictures are presented, in which all the elements that must be segmented can be seen: walls (pia mater and dura mater), nerve roots, blood vessels and lumen. In particular, the second image will be referred to in the following of the paper to make the description of the different phases of the algorithm clearer.



(a) Endoscopic image of the pia mater and a blood vessel.

(b) Endoscopic image used as example in the algorithm description. In particular, a blood effusion and a nerve are visible.

Fig. 1. Two examples of spinal subarachnoid endoscopic images.

The segmentation process consists of several phases, as represented in fig.2.

An adaptive histogram based segmentation is first applied to the luminance component of the input image, looking for the (dark) lumen. Several non-connected regions might be labeled as lumen because of possibly present vessels or nerves. If the size of at least one of the regions labeled as "lumen" is wide enough, the overall shape of the lumen is reconstructed and a search for nerve roots is performed inside the lumen-labeled region. If not, a search for a brighter and veiled region (called *dirty lumen*) is performed: for a deeper description of this concept, see sect.II-E.

In the next step a segmentation on the Hue and Saturation components of the input image is performed, and used together

with the previously segmented image for the isolation of possibly present blood vessels in the lumen region.

In the following, each phase is described in detail: the titles of the paragraphs and the names of the corresponding boxes in the flowchart of fig.2 are the same.

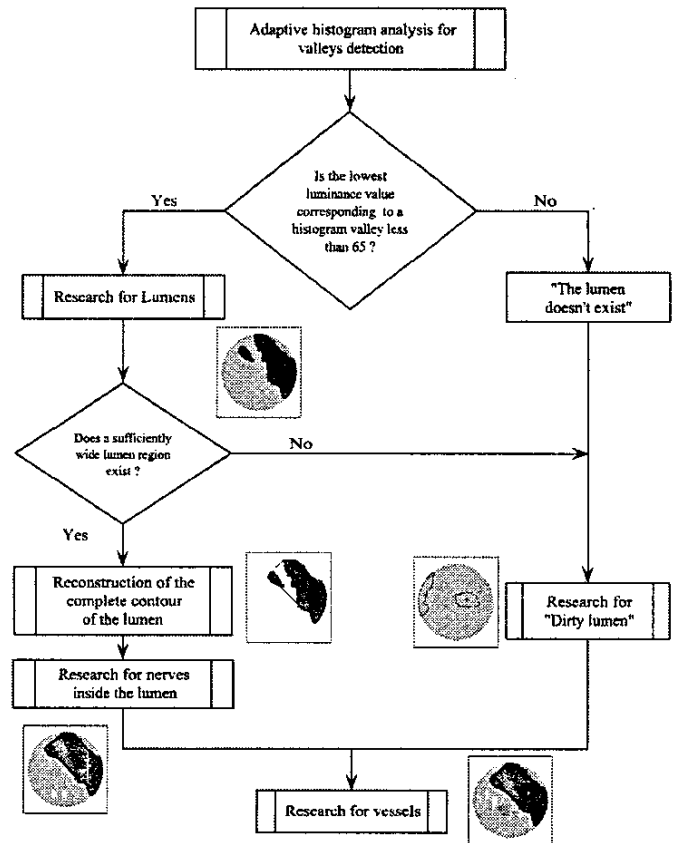


Fig. 2. Flow diagram of the segmentation algorithm

A. Adaptive histogram pre-processing

The histogram of the luminance component of the image is computed, and a smoothing average filter (on a five pixel long sliding window) is applied to it. The averaged histogram will be referred to in the following by the notation $h[i]$ (i is the gray level, from 0 to 255). $h[i]$ for the example input image is reported in fig.3(a).

Local minima are then looked for in $h[i]$ [11]: the luminance level i corresponds to a local minimum iff

$$(h[i] < h[i - 1]) \text{ AND } (h[i] \leq h[i + 1])$$

The particular combination [$<$; \leq] of logical operators in the previous condition comes from the imperative of not over-estimating the detected lumen size: in fact the aim of this histogram analysis phase is to extract a list of significant local minima, and among them to choose the most indicated one for thresholding the image. For safe navigation purposes, it would

be very dangerous to over-estimate the size of the lumen, much better to consider it smaller than the real one, so keeping the lowest thresholding level among a list of equally valued local minima. In fig. 3(b) the minima found up to this phase are visible.

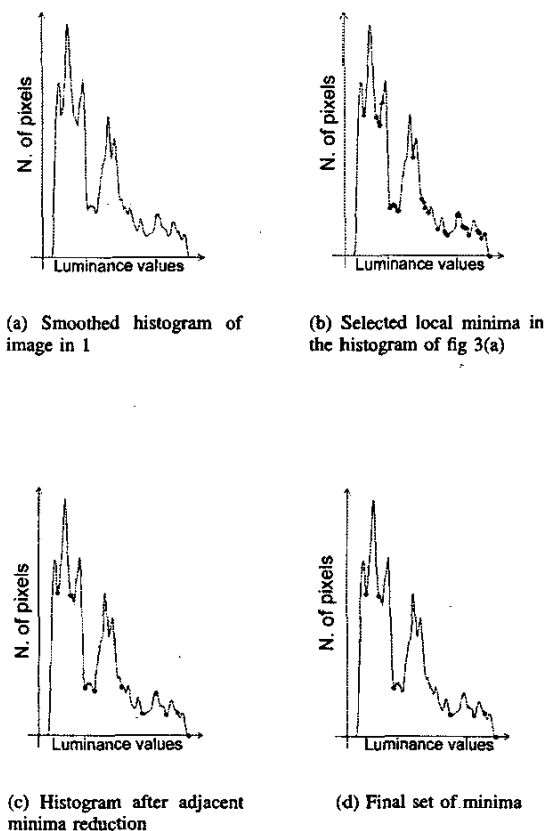


Fig. 3. Phases of the lumen finding process

In the following, the process of lowering the number of minima is described. Let's define $mins[k]$ the dynamic vector containing the luminance value of the local minima of $h[i]$.

If two adjacent minima are separated by no more than 15 units on the luminance axis, only one of them must survive ([11]) and classical algorithms save the lowest; our approach is to keep the minimum whose index is $mins[k]$ if the condition

$$h[mins[k]] \leq 0.85 \cdot h[mins[k-1]] \quad (1)$$

is verified: if not, the index $mins[k-1]$ is kept. The reason of this choice is once more to keep as low as possible the possibility of overestimating the size of the lumen. In fig.3(c) the behavior of this processing phase on the histogram in fig.3(a) is shown.

The attention is then posed on possible peaks between two adjacent local minima. Between two valleys there is a peak if

the condition

$$\frac{(h[mins[k-1]] + h[mins[k]])/2}{havg} \leq 0.75 \quad (2)$$

is satisfied [11], where $havg$ is the average value of the pixels between the two valleys. If a peak is present, the index $mins[k-1]$ is kept; if not, a condition on the two amplitudes states which one of the two valleys has to be kept: if

$$h[mins[k]] \leq 0.85 \cdot h[mins[k-1]] \quad (3)$$

$mins[k-1]$ is eliminated: this is the case when there are much less pixels having intensity $mins[k]$ than those having intensity $mins[k-1]$.

In fig.3(d) the dots correspond to the final valley set used in the following segmentation phases.

B. Research for lumens

The input image is binarized using as threshold the highest valley whose luminance value is less than 65. This value has proven to be the most adapt for many endoscopic images. Morphological opening and closing operations are applied to remove small white and black areas. The gray level of the binarized image is used as homogeneity criterion for a region growing segmentation algorithm [13]. A region of adjacent pixels satisfying the homogeneity criterion is called *blob*. The blobs corresponding to the lumen are isolated; blobs whose size is less than a given fraction of the input image size are discarded.

If the size of any of the isolated lumen blobs is big enough, the lumen is said to be "non-existent" and the algorithm looks for a possible "dirty lumen" (see sect. II-E).

If some blobs labeled as *lumen* have been isolated, the next step is the reconstruction of the whole lumen shape. In fig.4(b) the regions segmented as lumen are shown in black, with respect to the original input image in fig.4(a).

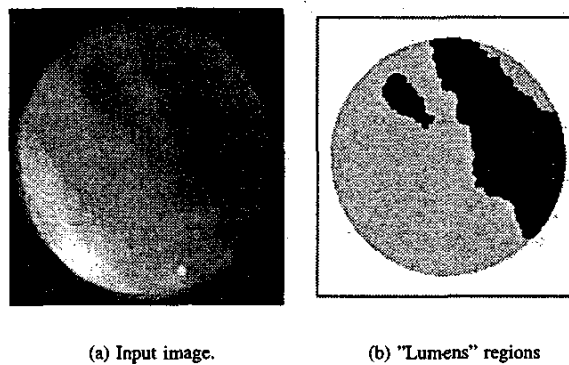


Fig. 4. First segmentation step

Once the lumens have been recognized, several approaches can be followed to recognize nerves, vessels, and walls.

At first, we have attempted to segment the image using combinations of luminance and hue [11] characteristic of the different structures listed above, without success.

An edge-based segmentation [14] failed because of common features of subarachnoid endoscopic images: they show very smooth edges, and boundaries between different areas are often very difficult to detect.

A three step hybrid approach has then been implemented to overcome these difficulties: all the regions labeled as lumen are connected, and the segmentation starts from this area; then nerves are isolated inside this region; the outer regions are labeled as *walls*; at the end blood vessels are detected.

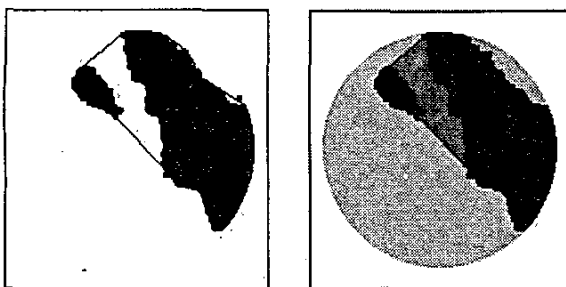
C. Reconstruction of the complete contour of the lumen

In order to find the overall lumen shape in spite of the possible structures that can partially occlude it (see sect: II-B), a morphological algorithm has been developed; it is a simplified and modified implementation of the "Convex Hull" algorithm, whose roots can be found in the computational geometry [15].

In the bi-dimensional case, "Convex Hull" algorithms determine, given a set of points P , the smallest 2D convex polygon that contains all the points in P . In our case the set P can be made up of the boundary points of all the regions labeled as lumen.

As already said, the overall lumen in subarachnoid endoscopic images can often show a certain degree of concavity, due to the anatomy of the space. This seems to be in contrast with the algorithm used for its reconstruction: since the concavity, for the same anatomic reasons, can never exceed a given (low) value, the Convex Hull algorithm was modified so as to allow a given amount of concavity in the lumen shape.

The computational complexity of the original Convex Hull ($O(n \log(n))$) is not compatible with a real-time implementation. A faster approximated implementation has been chosen (see [15]); moreover the border has been sub-sampled for even faster execution. The computational cost of the implemented algorithm is $O(n)$.



(a) Complete lumen reconstructed by the Modified Convex Hull algorithm

(b) Segmented image in which walls (in white), lumen (in black) and nerve (in gray) are visible

Fig. 5. Second and third segmentation steps: complete lumen and nerve root.

As already said, the lumen could be slightly concave, not only for anatomical reasons: the local concavity could also

be due to artifacts caused by reflections of the structures around the lumen. For these reasons the condition that controls the convexity of the region being built has been relaxed. A parameter of the algorithm controls the amount of concavity that can be tolerated. An example of concave lumen contour is visible in fig.5(a).

D. Research for nerves inside the lumen

With respect to the same picture, the white blobs are looked for; since the lumen's contour has been depicted in black, the white blobs which fall inside the lumen outline are recognized as distinct from the white blob who falls outside the lumen outline (labeled as "wall"). A selection on the white regions internal to the border discards all the regions whose size is less than a given fraction of the input image size. The remaining blobs are labeled as nerves. It is a temporary labeling, because some of them, in the next segmentation phase, could be identified as vessel (see sect.II-F).

In figure 5(b) the extracted nerve is visible in gray.

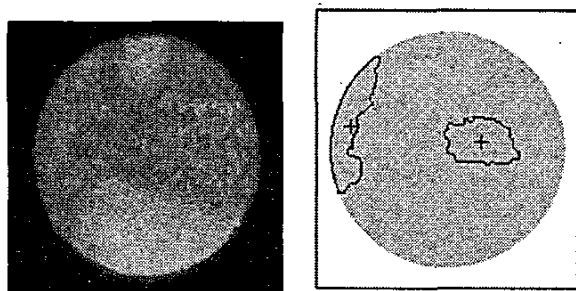
E. Research for the "Dirty lumen"

Many of the images processed by the authors during subarachnoid spinal endoscopies are blurred, due to both semi-transparent structures lying in front of the endoscope camera and the presence of unpredictable disturbing reflections. In such a context, the lumen often appears much more bright than in the clearly visible images, with brightness levels usually owned by nerves, walls and veins, so that it is not always possible to extract the lumen regions by using the method described in the section (see sect:II-B)

The adopted solution is to perform a thresholding operation with threshold values slightly greater than those employed for the detection of clear lumens. In particular, threshold is given by the greatest luminance value among those less than 130 contained in $mins[k]$. In this manner, even if the value 130 is fixed, an adaptive behavior that depends on the result of the luminance histogram analysis is obtained. Then the regions extracted from the image are, made more homogeneous by means of opening and closing operations. Among all the selected regions, only those with a sufficiently wide area are considered. For a given image, we say that the dirty lumen exists only if at least one image portion which passes the above mentioned selections is found.

It is important to notice that we do not give any label to the selected dirty lumen. It is as if the algorithm asked for further information on a particular region which has not been recognized but that could reveal, by making some advancement of the catheter, the existence of a lumen. It is a suggestion for the future direction of the catheter.

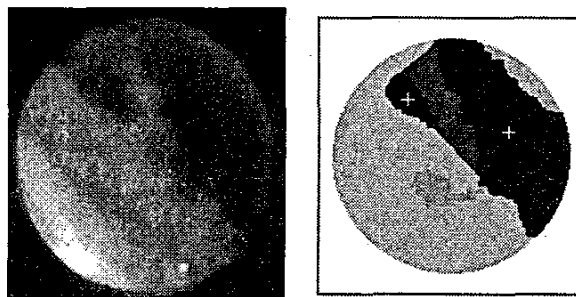
As the endoscopic image used as example in the paper has a clearly visible lumen, the dirty lumen detection has been shown by introducing another endoscopic image, presented in fig.6(a). The black contour drawn in fig.6(b) represents the perimeter of the detected dirty lumen region.



(a) Sample input image.

(b) Region labeled as "Dirty Lumen"

Fig. 6. Example of the behavior of the algorithm in presence of not well defined images



(a) Original input image.

(b) Completely segmented image.

Fig. 7. Last step of the segmentation process.

F. Research for vessels

The extraction of the vessels can be accomplished by searching for the red portions of the endoscopic image. The HLS color space has been used, as usual when the human perception of the colors is involved in the processing ([16], [17]).

In our approach, both the Hue and the Saturation components of the input image have been used; in fact, since the vessels in endoscopic images are rarely pure-red colored and phenomena of reflexions of the camera light are common, a segmentation based uniquely on the Hue component is not sufficient.

After an examination of a vast set of endoscopic images, appropriate thresholds for the Hue and Saturation were chosen. The Hue has been used to capture all the small variations of red color usually present in a vessel, while the limitations introduced for the saturation are used to discard the regions having a not sufficient quantity of red. In fig.7(b) the extracted red portion of the sample endoscopic image is represented in light gray.

However, as the perceived color strongly depends on the reflection angles of the illuminating light ray on the vessel surface, the whole vessel region cannot sometimes be extracted. Reminding that in sec.II-D all the non-lumen regions which fall inside the lumen contour have been temporarily labeled as "nerve", it is possible, now, to verify if a significant spatial overlap between each one of these nerve-labeled regions and the extracted red portions exists. In particular, if the size of the overlapping region is larger than 90% of the "vessel" region, or larger than 40% of the "nerve" region, the particular area is given the label "vessel" and the area previously defined as "nerve" becomes "vessel".

III. EXPERIMENTAL RESULTS

The algorithm has been thoroughly tested on video streams from endoscopic explorations of animal (pig) spinal cords in vivo. Experimental results showed the complete accordance with classification made by medical doctors. Some of the

results have been shown in the previous pictures, in sect.II; other segmented images are reported in fig.8 and fig.9: in 8(a) two nerve fibers are detected inside the lumen, in which three non-connected "safe" navigation areas are isolated; in 8(b) a blood vessel runs along the dura mater; lumen is detected as well; in 9(a) and 9(b) images are too blurred to "safely" detect lumen, and the the blue-bordered area is labeled as "dirty lumen"; in 9(a) a vessel is detected. In these images the white cross indicates the centroids of the "lumen" or "dirty lumen" segmented regions.

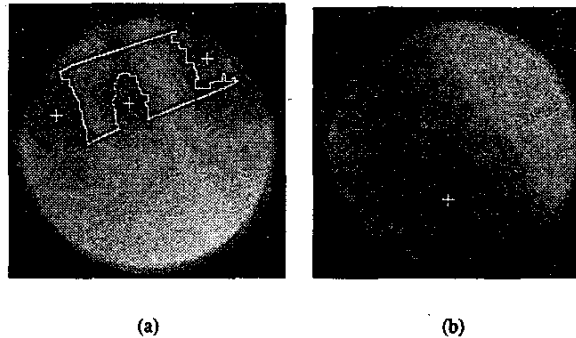


Fig. 8. Samples of segmented endoscopic images (1).

Experimental trials of the whole robotic system have been conducted during the mentioned ex-vivo and in-vivo experiments.

The implemented version of the algorithm draws borders over the original image, to help in realizing an "augmented-reality" environment. In fig.10 is reported a screenshot of the display during a real endoscopy on a pig.

The proposed algorithm has proven to have good performances in terms of both accuracy in the segmentation of images and computation time.

The computing system was composed of a desktop PC equipped with a Matrox "Orion" frame-grabber and "Matrox

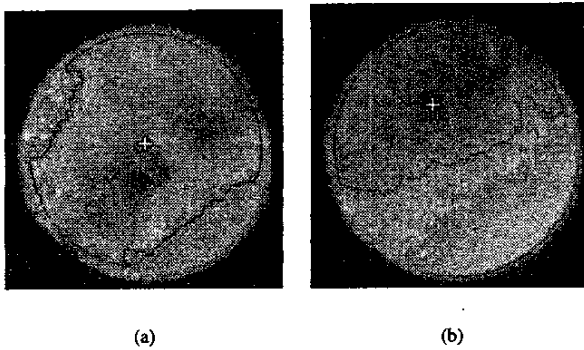


Fig. 9. Samples of segmented endoscopic images (2)

Imaging Libraries". The time needed for segmenting the input image is around 60ms.

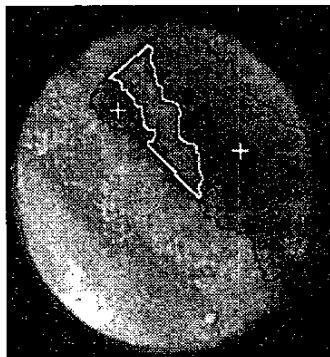


Fig. 10. Segmentation borders superimposed to the input image.

IV. CONCLUSION AND FUTURE WORK

We proposed a multi-step adaptive algorithm for segmenting endoscopic images of the spinal sub-arachnoid space.

It is the first module of an assisted navigation system for the exploration of the human sub-arachnoid space. Due to the extremely delicate structures present, the constraints in terms of safety are strong: the algorithm has proven to have a defined and predictable behavior in almost all the situations a normal endoscopy can present.

Our next step is the application of the algorithm in support of the navigation, in order to provide the system with a perception of the three-dimensional environment: vessels, nerves and walls have to be perceived in a 3-D space, in order to assure a safe behavior and to provide the surgeon with an effective help in avoiding dangerous collisions.

ACKNOWLEDGMENT

This work is being carried out under the european project Mi.N.O.S.C. (MicroNeuroendoscopy of Spinal Cord - contract N. QL65-CT-2001-02150), in the framework of the "Quality of Life and Management of Living Resources" Program. The authors would like to thank the European Commission for co-funding the project.

The authors would like to thank Dr. Oliver Tonet and Dr. Giuseppe Megali for the helpful discussions during the work.

REFERENCES

- [1] L. Saberski and P. Dickey, "Spinal canal endoscopy," *Min Invas Ther & Allied Technol* 1998:7/2:119-122, pp. 119-122, 1998.
- [2] D. Chatenever, "Minimally invasive surgical visualization- past, present, and future," *J. Minim. Invasive Spinal Tech.*, 2001.
- [3] J. Warnke, M. Tschabitscher, and A. Nobles, "Thecaloscopy: the endoscopy of the lumbar subarachnoid space, part 1: Historical review and own cadaver studies," *Minim. Invas. Neurosurgery*, pp. 61-64, 2001 (44).
- [4] L. Ascari, C. Stefanini, A. Menciassi, S. Sahoo, P. Rabischong, and P. Dario, "A new active microendoscope for exploring the sub-arachnoid space in the spinal cord," in *Proceedings of the 2003 International Conference on Robotics and Automation (ICRA)*, 2003.
- [5] C. Kwok and D. Gillies, "Using fourier information for the detection of the lumen in endoscope images," *Proc. IEEE Tencon (IEEE Region 10's Ninth Annual International Conference)*, pp. 981-985, 1994.
- [6] G. Khan and D. Gillies, "Vision based navigation system for an endoscope," *Image and Vision Computing* 14 (1996), pp. 763-772, 1996.
- [7] K. Asari, Srikanthan, S. T. Kumar, and D. Radhakrishnan, "A pipelined architecture for image segmentation by adaptive progressive thresholding," *Microprocessors and Microsystems* 23 (1999), pp. 493-499, 1999.
- [8] K. Asari and T. Srikanthan, "Segmenting endoscopic images using adaptive progressive thresholding: a hardware perspective," *Journal of Systems Architecture* 47 (2002), pp. 759-761, 2002.
- [9] S. Kumar, K. Asari, and D. Radhakrishnan, "A new technique for the segmentation of lumen from endoscopic images by differential region growing," *IEEE (1999)*, pp. 414-417, 1999.
- [10] K. Asari, "A fast and accurate segmentation technique for the extraction of gastrointestinal lumen from endoscopic images," *Medical engineering & physics* 22 (2000), pp. 89-96, 2000.
- [11] M. Tjoa, S. Krishnan, C. Kugean, P. Wang, and R. Doraiswami, "Segmentation of clinical endoscopic image based on homogeneity and hue," *IEEE Proceedings of the 23rd Annual EMBS International Conference*, pp. 2665-2668, 2001.
- [12] S. Krishnan, X. Yang, K. L. Chan, and P. Goh, "Region labeling of colonoscopic images using fuzzy logic," *Proceedings of The First Joint BMES/EMBS Conference Serving Humanity, Advancing Technology*, p. 1149, 1999.
- [13] P. Wang, S. Krishan, Y. Huang, and N. Srinivasan, "An adaptive segmentation technique for clinical endoscopic image processing," *Proceedings of the second joint EMBS/BMES Conference*, pp. 1084-1085, 2002.
- [14] M. Sonka, V. Hlavac, and R. Boyle, *Image Processing, Analysis, and Machine Vision*. PWS Publishing, 1999.
- [15] F. Preparata and M. Shamos, *Computational Geometry. An Introduction*. Springer-Verlag, 1985.
- [16] Q.Huynh-Thu, M.Meguro, and M.Kaneko, "Skin-color extraction in images with complex background and varying illumination," *Proceedings of the Sixth IEEE Workshop on Applications of Computer Vision*, 2002.
- [17] J.R.Smith and S.-F. Chang, "Single color extraction and image query," *IEEE*, pp. 528-531, 1995.